

Rates and patterns of urban expansion in China's 32 major cities over the past three decades

Shuqing Zhao · Decheng Zhou ·
Chao Zhu · Wenyuan Qu · Jiajia Zhao · Yan Sun ·
Dian Huang · Wenjia Wu · Shuguang Liu

Received: 1 December 2014 / Accepted: 8 May 2015 / Published online: 15 May 2015
© Springer Science+Business Media Dordrecht 2015

Abstract

Context Rates, patterns, and consequences of urban expansion are drawing increasing attention globally because of their profound impacts on socioeconomics, human life, and the environment. Horizontal comparative studies across multiple cities over large geographic regions are rare.

Objectives We quantified and compared the magnitude and forms of urban expansion for China's 32 major cities, and examined the spatiotemporal evolution of urban growth and trajectory of patch structure formation.

Methods Multi-temporal Landsat data of circa 1978, 1990, 1995, 2000, 2005, and 2010, patch-based analyses, and urban growth metrics were used.

Results These 32 major cities have experienced extensive expansion during the study period. Leapfrogging was the dominant urban expansion form,

followed by edge-expansion and infilling in the early time periods. Interestingly, the fractions of infilling, edge-expansion, and leapfrogging has gradually reached a quasi-equilibrium condition with a ratio of 2:4:4 (the number) and 2:5:3 (the area) during recent years. Patch analysis suggested that these cities evolved under a nationally-consistent converged urban patch structure regardless of city size, location, and history. The dynamics of urban growth in China corresponded well with its socioeconomic and political geography and the phased implementation of various regional and national policies.

Conclusions Our results generally supported the continuum of diffusion-coalescence urbanization process and a spatial self-organization of urban land patches during urbanization. More studies are needed to test the generality of urban growth hypothesis and examine the universality of converged urban patch structure across regions and countries and to understand their implications to city organization, metabolism, and evolution.

Electronic supplementary material The online version of this article (doi:10.1007/s10980-015-0211-7) contains supplementary material, which is available to authorized users.

S. Zhao (✉) · D. Zhou · C. Zhu · W. Qu ·
J. Zhao · Y. Sun · D. Huang · W. Wu
College of Urban and Environmental Sciences, and Key
Laboratory for Earth Surface Processes of the Ministry of
Education, Peking University, Beijing 100871, China
e-mail: sqzhao@urban.pku.edu.cn

S. Liu
Geospatial Science Center of Excellence (GSCE), South
Dakota State University, Brookings, SD 57007, USA

Keywords Urbanization · Spatiotemporal dynamics · Remote sensing · Urban growth modes · Patch structure · Self-organization

Introduction

The world is increasingly urban through accelerating urbanization and a majority of people now reside in

urban areas (UN 2013). Urbanization, characterized primarily by dramatic demographic shift from rural to urbanized areas and physical urban land expansion, poses both opportunities and challenges for the sustainability transition toward long-term balances between human needs and the planet's environmental capacities (Seto et al. 2010; Wu et al. 2013). Knowledge spillovers, innovation, and wealth creation generally scale super linearly with population size (increasing returns) (Lucas 1988; Bettencourt et al. 2007). On the other hand, physical urban expansion, replacing natural vegetation or crops with impervious surfaces as cities grow, is probably the most drastic, widespread, and irreversible form of land transformation on Earth surface (Tan et al. 2005; Radeloff et al. 2010). The impacts of urban expansion extend far beyond its physical boundaries in many dimensions (Folke et al. 1997; Grimm et al. 2008) including loss of arable land (Tan et al. 2005), loss of biodiversity and habitats (McKinney 2002; McDonald et al. 2008; Seto et al. 2012), degradation of water and air quality (Shao et al. 2006; Zhao et al. 2006; Chen et al. 2011; Deng et al. 2012), alteration of local and regional climate (Kalnay and Cai 2003; Zhou et al. 2004; Zhao et al. 2006; Trusilova et al. 2008; Yang et al. 2011) and biogeochemical cycles (Seto et al. 2012; Zhang et al. 2012).

As an inevitable process, urbanization will present profound impacts on socioeconomics, human life, and the environment in the twenty first Century. As such, how and where urbanization develops is an urgent challenge for the transition toward sustainability (Bettencourt et al. 2007; Grimm et al. 2008). However, most of our understanding of urbanization at regional and global scales is based on the knowledge of dramatic demographic changes (e.g., Montgomery 2008; Seto et al. 2010). Our current knowledge on the extents, rates, forms, driving forces, consequences, and geographic similarity and differences of urban expansion is limited (Seto et al. 2011). Previous studies focused mostly on individual cities (e.g., Seto and Fragkias 2005; Tian et al. 2011; Wu et al. 2011; Ernoul et al. 2012), and horizontal comparative studies across multiple cities over large geographic regions are sorely lacking (Angel et al. 2005; Schneider and Woodcock 2008; Frohking et al. 2013; Schneider and Mertes 2014). Therefore, characterizing spatially explicit patterns and forms of urban expansion at regional and global scales is the fundamental first step

to understand urbanization itself, its diverse impacts, and then contribute to the development of general urbanization theories that can be used to support a sustainable urban future (Seto et al. 2011; Wu et al. 2011; Wu 2014).

China has experienced rapid urbanization in parallel with its economic boom over the past three decades: from only 17.9 % of country's population living in cities in 1978 to more than 50 % in 2011 (SSB 2012). Many studies, with most on individual or a few cities on the eastern coastal areas, have been conducted to characterize China's urbanization (e.g., Weng 2002; Zhao et al. 2006; Xu et al. 2007; Lv et al. 2011; Li et al. 2013a; Sun et al. 2013). Several attempts have been made to investigate the urban expansion processes across China using Landsat images (Ji et al. 2001; Liu et al. 2005; Wang et al. 2012; Schneider and Mertes 2014). However, large uncertainty remains even on the overall rate of change, let alone the spatial and temporal patterns and driving forces. For example, Liu et al. (2005) found that China's urban land expanded 8,170 km² between 1990 and 2000, which was 17 % lower than the estimate by Wang et al. (2012) for the same period, and 47 % lower than the estimate of 12,000 km² for a shorter time period (from 1989/1992 to 1996/1997) (Ji et al. 2001). Schneider and Mertes (2014) recently provided a more comprehensive view of urban expansion for 142 Chinese cities from 1978 to 2010. However, their analyses did not cover all the official administrative areas for each city, and the rates, spatial patterns and forms, temporal courses, and major driving forces of urban expansion across China remained largely unexplored.

In this study, we mapped and quantified the rates, spatial patterns and forms, and temporal courses of urban expansion for 32 major cities based on their administrative boundaries across China over the past three decades using multi-temporal Landsat Multispectral Scanner (MSS), Thematic Mapper (TM) and Enhanced Thematic Mapper (ETM) data of circa 1978, 1990, 1995, 2000, 2005, and 2010. The objectives of this study were to (1) map the spatial and temporal dynamics of urban land covers in 32 cities, (2) quantify and compare the magnitude and forms of urban expansion for 32 cities, and (3) analyze the characteristics of urban land patches for 32 cities, and convergence or divergence of urban patch structure in China.

Data and methods

Remote sensing of urban land covers

Our study covered 32 major cities including municipalities, provincial/autonomous regional capitals, and the city of Shenzhen. Shenzhen, the first Special Economic Zone established in 1978 by the Chinese government, was included because it is now considered one of the fastest growing cities in the world. The boundaries of these 32 major cities were defined according to China's official definition of their administrative areas (i.e., city, *shi*) (Chan 2007) (Fig. 1).

Mapping urban extent over large areas demands a consistent and unambiguous definition of “urban area”. Various definitions, dependent more on input data sources than on methodology, have been used in the past, resulting in diverse estimates on the extent of urban area (Schneider et al. 2009). In this study, urban land was defined as all non-vegetative areas dominated by human-made surfaces (e.g., roads and buildings), including residential, commercial, industrial, and transportation space, following the definitions and practices of most studies (Elvidge et al. 2007; Schneider et al. 2009; Bai et al. 2012). Urban land can therefore be considered interchangeable with impervious surface or the built environment.

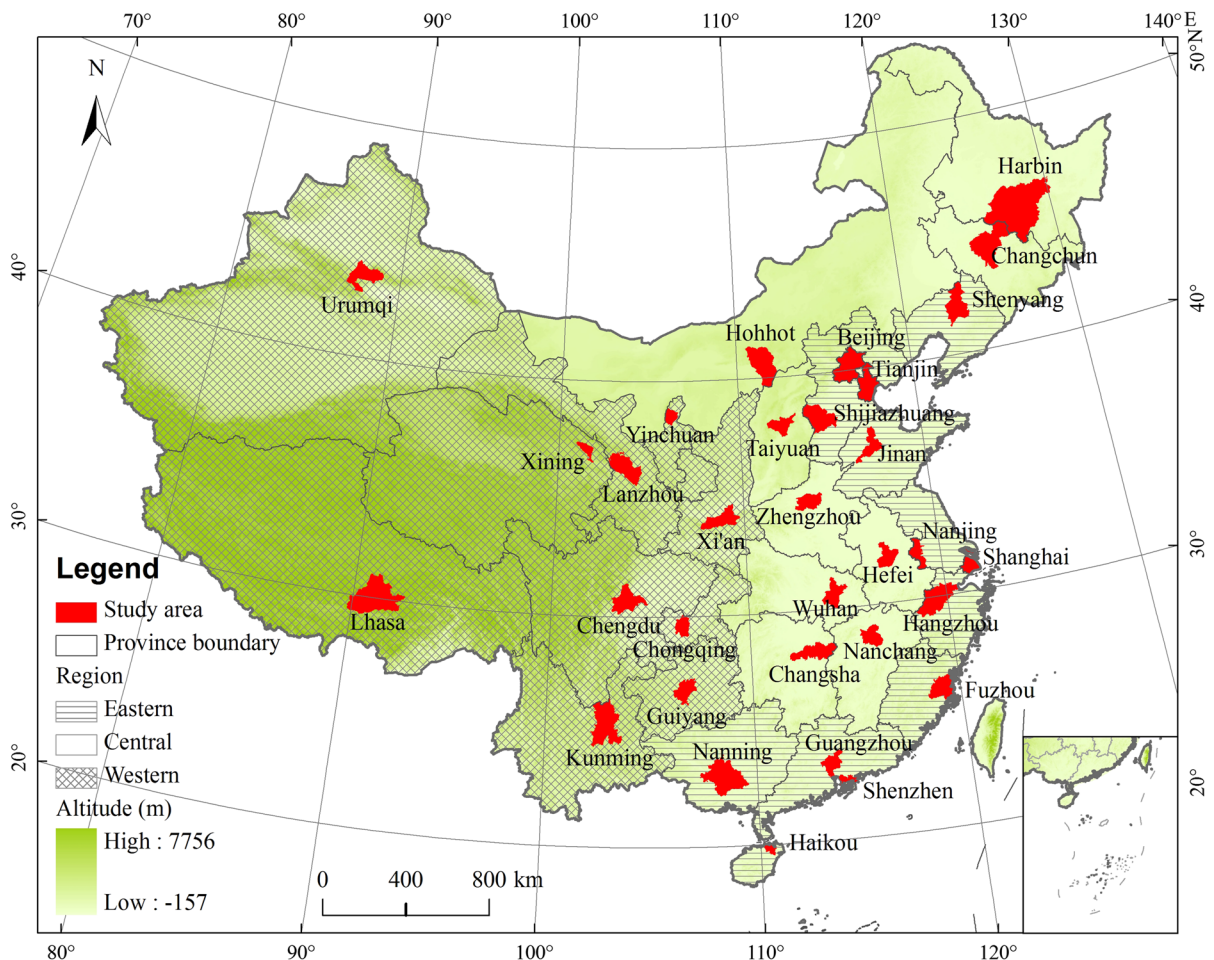


Fig. 1 The administrative boundaries of 32 major cities in China. They include municipalities, provincial/autonomous regional capitals, and the city of Shenzhen. Shenzhen, the first Special Economic Zone established in 1978 by the Chinese government, was included because it is now considered one of

the fastest growing cities in the world. The background map shows the topography of China. Three geographic divisions in China, eastern, central and western regions based on Lin (2002) are illustrated

Cloud-free Landsat Multispectral Scanner (MSS), Thematic Mapper (TM) and Enhanced Thematic Mapper (ETM) remote sensing imageries were used to obtain the information on urban land expansion for those 32 cities over the past three decades. We collected over one thousand scenes of images and around 500 with relatively high-quality were used to extract the extent of urban land for all the cities in this study (Table S1). Most of the selected images were acquired during summer in order to separate urban areas from certain crop fields that might be spectrally similar to urban areas in a spring image (Yuan et al. 2005). The acquisition time of these images spanned 1973–1981, 1988–1992, 1994–1996, 1999–2001, 2004–2006, and 2009–2010 (Fig. S1), nominally representing six time periods of circa 1978, 1990, 1995, 2000, 2005, and 2010, respectively. The time span corresponds to the period of rapid urbanization in China since the initialization of the national policy of “reform and opening-up” in the late 1970s (Lin 2002). In most cases, several images acquired at different dates have to be mosaicked to cover a city (Table S1). As a convention (Bagan and Yamagata 2012), the nominal date of the mosaicked Landsat image was the date of the Landsat image that covered most of the urban area for each time period (Fig. S1).

Landsat MSS, TM, and ETM data were pre-processed (e.g., re-projection, mosaic, histogram equalization) using ERDAS Imagine version 9.2. Albers Conical Equal Area was used as the re-projection coordinate system and all the images were resampled to the resolution of $30\text{ m} \times 30\text{ m}$, resulting in a minimum mapping unit or minimum patch of urban land area of 900 m^2 . The images in 1978, 1990, 1995, 2005, and 2010 were geo-encoded and matched to the image in 2000 with the error of less than half-pixel for each city.

The land covers were classified into four broad types (i.e., cropland, urban land, water body, and other land cover) using the maximum likelihood classification (MLC) approach (Zhao et al. 2006). As defined previously, urban land consisted of all non-vegetative areas dominated by human-made surfaces (e.g., roads and buildings), including residential, commercial, industrial, and transportation space. Water bodies included the reservoirs, ponds, and rivers. The other land cover category included forest, shrub, grass and bare land. We integrated the histogram-equalized

NDVI (derived from the Landsat images) and Digital Elevation Models (DEM, downloaded from <http://www.gdem.aster.ersdac.or.jp/search.jsp>) into our classification. This has often been regarded as an effective method for enhancing the spectral and topographic differences across various land covers, and thus could improve the classification accuracies (Stefanov et al. 2001; Pedroni 2003; Saha et al. 2005).

Post-classification refinements were applied to reduce classification errors caused by the similarities in spectral responses of certain classes such as bare fields and urban and some fallow agricultural land based on expert knowledge (Yuan et al. 2005; Jat et al. 2008). Ancillary information from various sources (e.g., DEM, Chinese vegetation map (<http://westdc.westgis.ac.cn>), land covers in different time periods, and local residents) was integrated to refine the classification results. As our main focus was on characterizing urban expansion, the land covers were further aggregated into two categories: urban land and non-urban land (i.e., cropland, water body, and the other land cover). Due to the resolution limitation of remote sensing images, it is difficult to distinguish small isolated urban pixels from non-urban patches, which may lead to some biases of the classification results. To reduce this effect, a $1\text{ km} \times 1\text{ km}$ moving window was used to generate urban land intensity, defined as the percentage of urban land pixels at $30\text{ m} \times 30\text{ m}$ resolution within each $1\text{ km} \times 1\text{ km}$ grid. The urban pixels with urban land intensity less than 5% in a $1\text{ km} \times 1\text{ km}$ moving window were then excluded from urban land category.

The accuracies of the classified products were assessed using Google Earth Pro[®] (GE) (Luedeling and Buerkert 2008; Zhou et al. 2012). GE covers high resolution images (e.g., QuickBird, IKONOS, or SPOT5) for recent years over all the cities in this study. Additionally, some field photos were uploaded to Panoramio (<http://www.panoramio.com/>) which can help distinguish different land cover types. Because the high-resolution images were unavailable for the years before 2000 for all the areas and the years before 2009 for some areas, we used the images that were acquired in 2010 in GE to validate the accuracies of (1) the classification results of 2010, and (2) the classification results before 2010 in the areas only where land cover remained unchanged from 1978 to 2010. Two sets of 300 points were sampled over the classification results of 2010 and the unchanged areas

from 1978 to 2010 for each city, and these points were then imported into GE and superimposed over the high-resolution images for accuracy assessment. The Kappa coefficients measuring classification accuracy (Foody 2002) were calculated. Results showed that the Kappa coefficients of urban land for all cities were higher than 0.77 for the classification results of 2010 and more than 0.82 for the results before 2010, respectively (Table S2), which met the accuracy requirement of land cover change evaluation (Janssen and van der Wel 1994).

Rates and spatiotemporal analyses

The annual urban expansion rate (AER) of each city between five neighboring periods from 1978 and 2010 was calculated following the method of Seto et al. (2011), which converted urban expansion into a standard metric removing the size effect of urban land to facilitate the comparison across various cities:

$$\text{AER} = 100 \% \times \left(\sqrt[d]{\frac{U_{\text{end}}}{U_{\text{start}}}} \right) - 1 \quad (1)$$

where U_{start} is the urban area at the initial time, U_{end} the urban area at the end time, and d the time span of the period in years.

Three types of spatial analysis were performed in this study. First, urban expansion patterns and processes were examined by classifying urban growth into infilling, edge-expansion, and leapfrogging (Xu et al. 2007; Li et al. 2013a). Edge-expansion or urban fringe development refers to the newly developed urban area spreading out from the fringe of existing urban pixels; infilling denotes non-urban land that is surrounded by urban land underwent a change to urban land; leapfrogging denotes the new urban patch is developed without spatial connection to the existing urban land. To differentiate these three types, an urban expansion type (E) index was first quantified using following equation after overlapping consecutive urban land maps:

$$E = \frac{L_{\text{com}}}{P_{\text{new}}} \quad (2)$$

where P_{new} is the perimeter of a newly developed urban patch, and L_{com} is the length of common edge of this newly developed urban patch and existed urban

patch or patches. The value of E ranges from 0 to 1. Urban expansion type is defined as infilling when $E > 0.5$, edge-expansion when $0 < E \leq 0.5$, and leapfrogging when $E = 0$.

Second, the spatial organization and fragmentation of urban land were studied using patch analysis. A patch is defined as a relatively homogeneous area that differs from its surroundings (Forman 1995). The area and perimeter of each urban land patch in each map were derived using ArcGIS 9.3 software. To investigate the composition and frequency distribution, the patches were binned into 13 patch size classes: 0–0.05, 0.05–0.25, 0.25–0.5, 0.5–1, 1–2, 2–5, 5–10, 10–20, 20–50, 50–100, 100–200, 200–500, and >500 km². Because the actual patch sizes in each bin are unevenly distributed to the lower end (i.e., the number of smaller patches is usually higher than the number of larger patches), the actual mean patch size for each of these bins was recalculated as the mean size of all the patches fallen into that bin. The frequency and its relationship with patch size were investigated in the study.

Finally, we used the compactness index (CI) to measure the overall coalescence of the newly developed urban patches. The compactness index was calculated as follows (Liu et al. 2010):

$$\text{CI} = \frac{1}{A} \sum_{i=1}^N A_i E_i \quad (3)$$

where N is the total number of newly developed urban patches, A is the total area of these newly developed urban patches, and A_i and E_i is the area and E value of the i th newly developed urban patch, respectively. E value is the urban expansion index ranging from 0 to 1. A larger compactness index suggests a more compact urban expansion, and a smaller one represents a more diffuse urban expansion.

To analyze the geographic patterns (variability and similarity) of urban distribution, expansion rates, and growth characteristics and to understand their regional driving forces, we used a broad regionalization scheme that divides China into eastern, central, and western regions (Fig. 1). This regionalization is widely considered representing the general patterns of population, economy, climate, and terrain of China (Lin 2002).

Results

Urban expansion

Figure 2 and S2 show the overall spatial patterns of urban expansion in the 32 cities individually and Fig. 3 summarizes the areas and rates of expansion by city and time period. All cities have experienced extensive urban expansion over the past three decades, and the magnitude of growth varied with city. In the late 1970s, the city Harbin, as an old industrial base of China, had the largest urban area (878 km²), followed by Beijing (801 km²), Tianjin (795 km²), Shijiazhuang (682 km²), and Changchun (658 km²). The urban land area of Shanghai, the country's most modern city, was only 312 km² in 1979. Comparatively, most cities in the west (e.g., Guiyang, Xining, Lhasa, Hohhot, and Yinchuan) had urbanized area less than 20 km².

Large geographic variation existed in city size and expansion rate across China (Fig. 3). For example, cities with urban area more than 200 km² in the late 1970s were more largely located in the eastern region: seven (i.e., Beijing, Jinan, Nanjing, Shanghai, Shenyang, Shijiazhuang and Tianjin) out of the 13 cities in the eastern region, three (Changchun, Harbin and Zhengzhou) out of nine cities in the central region, and none out of 10 cities in the western region. By 2010, the average size of urban land for the cities in the western region (386 ± 343 km²) (mean \pm standard deviation, hereafter) was still substantially less than their counterparts in the eastern and central regions ($1,422 \pm 845$ and $1,231 \pm 867$ km², respectively).

China's 32 major cities have experienced extensive urbanization over the past three decades with an average annual expansion rate of 6.8 ± 2.5 % (mean \pm standard deviation) between 1978 and 2010. The annual urban expansion rates for 32 cities ranged from 1.2 to 20.8, 1.1 to 20.8, 1.1 to 18.8, 1.8 to 16.7, and 3.8 to 15.4 % for the periods 1978–1990, 1990–1995, 1995–2000, 2000–2005 and 2005–2010. The annual expansion rates of four, ten, five, two and nine cities were higher than 10 % during these five periods, respectively (Fig. 3). Overall, the average annual expansion rates for 32 cities were 7.0 ± 4.4 , 8.2 ± 5.4 , 6.3 ± 4.0 , 5.3 ± 3.2 , and 8.3 ± 2.9 % for these periods, respectively. The highest urban expansion rates occurred in the periods 1990–1995 and 2005–2010, and the largest variability, as indicated by

both the standard deviation and CV, was observed during 1990–1995. Tianjin became the largest city in urban area (3,343 km²) in China in 2010, followed by Changchun (2,828 km²), Harbin (2,586 km²), Beijing (2,452 km²), and Shanghai (1,871 km²). In contrast, the western cities such as Lhasa, Xining, Lanzhou, and Guiyang were still relatively small (less than 200 km²). Particularly, the city Shenzhen, as China's first Special Economic Zone, experienced the most rapid urban expansion from 16 in 1978 to 753 km² in 2010.

Characteristics of urban land patches

Patch size and its number in a given city at a given time followed a strong “hockey-stick” log–log relationship (Fig. 4). The hockey stick graph is formed by a relatively straight log–log relationship when the frequency of patches were higher than one (i.e., hockey stick's “shaft”), followed by a sharp, steady increase in patch size with a frequency of one (corresponding to the “blade” portion). The blade portion is an important feature that usually characterizes the largest urban land patch in a city, often the urban center or core, and it does not follow the overall size–frequency relationship presented by the size bins with more than one patch. The largest patch size expanded over time and varied across cities (Table 1; Fig. 4).

The slopes of the hockey stick shaft sections (i.e., defined by the bins with more than one patch) across all cities and times varied within a narrow range [−1.62, −1.00] (95 % confidence interval represented by the 2.5 and 97.5 % quantiles) (Figs. 4, 5). In contrast, the intercepts varied greatly with a 95 % confidence interval being [−0.03, 2.02]. In general, the intercept increased over time, signifying the overall increase of patch numbers, for a given city (Fig. 4). Furthermore, the intercepts were strongly associated with the total urban land area (only accounted for the bins with more than one patch) across all cities (Fig. 5). From the log–log relationship between patch size (S , in km²) and its corresponding number (N) (Fig. 4), we have:

$$\log_{10}(N) = \alpha + \beta \cdot \log_{10}(S) \quad (4)$$

where the values of β varied narrowly around its mean, and α is a function of the total urban area (A , in km², excluding the bins with only one patch) (Fig. 5):

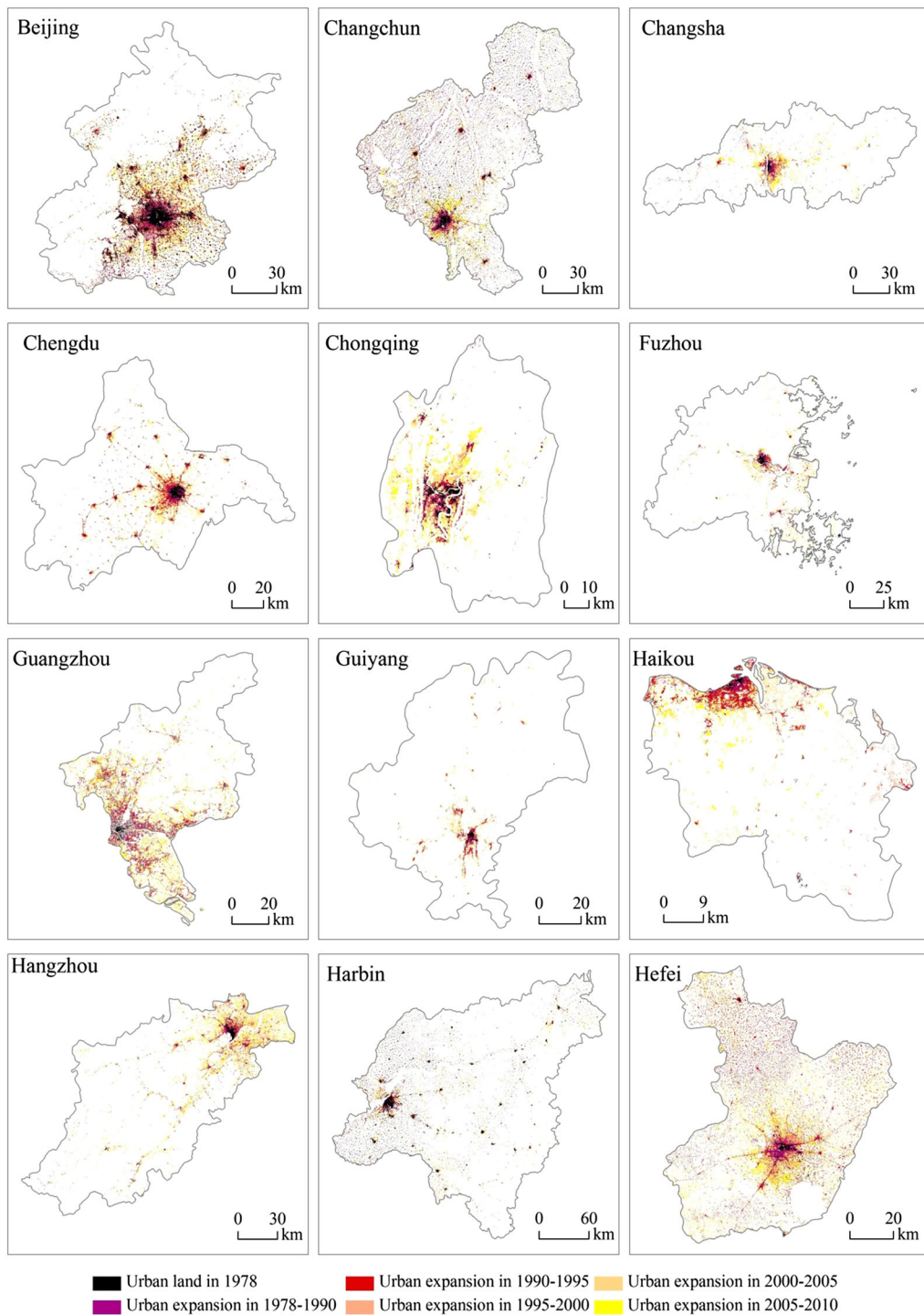


Fig. 2 Spatial distribution of urban expansion in selected cities in China over the past three decades. The outlines are their administrative boundaries. The rest of the 32 cities are shown in Fig. S2 in the Supporting Information

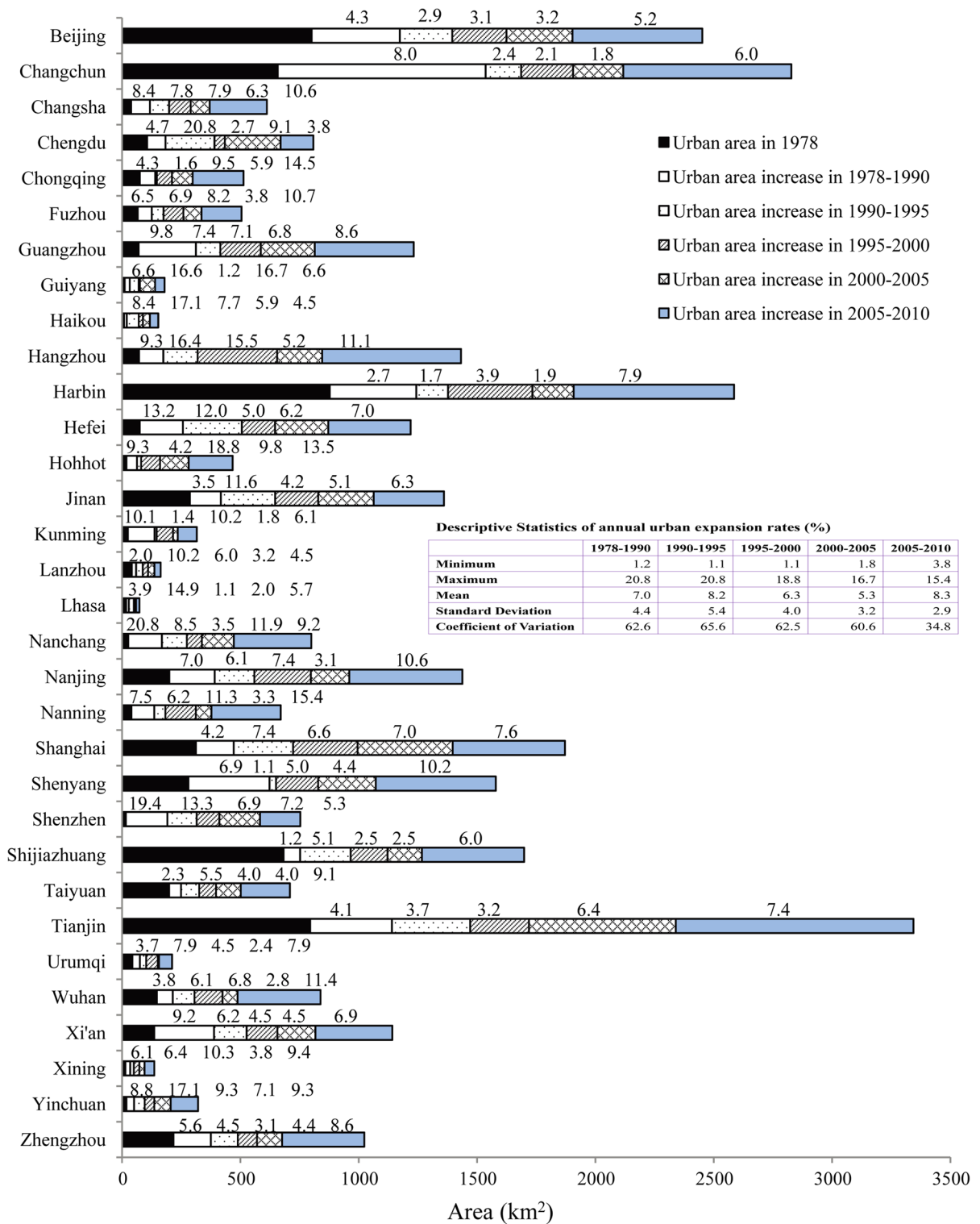


Fig. 3 The existed urban area in 1978 and the growth of urban area (km²) between five neighboring periods from 1978 to 2010 for 32 major cities in China. The normalized annual urban

expansion rates (%) among five neighboring periods are shown at the top of each bar correspondingly, and the insert table lists the descriptive statistics of annual urban expansion rates

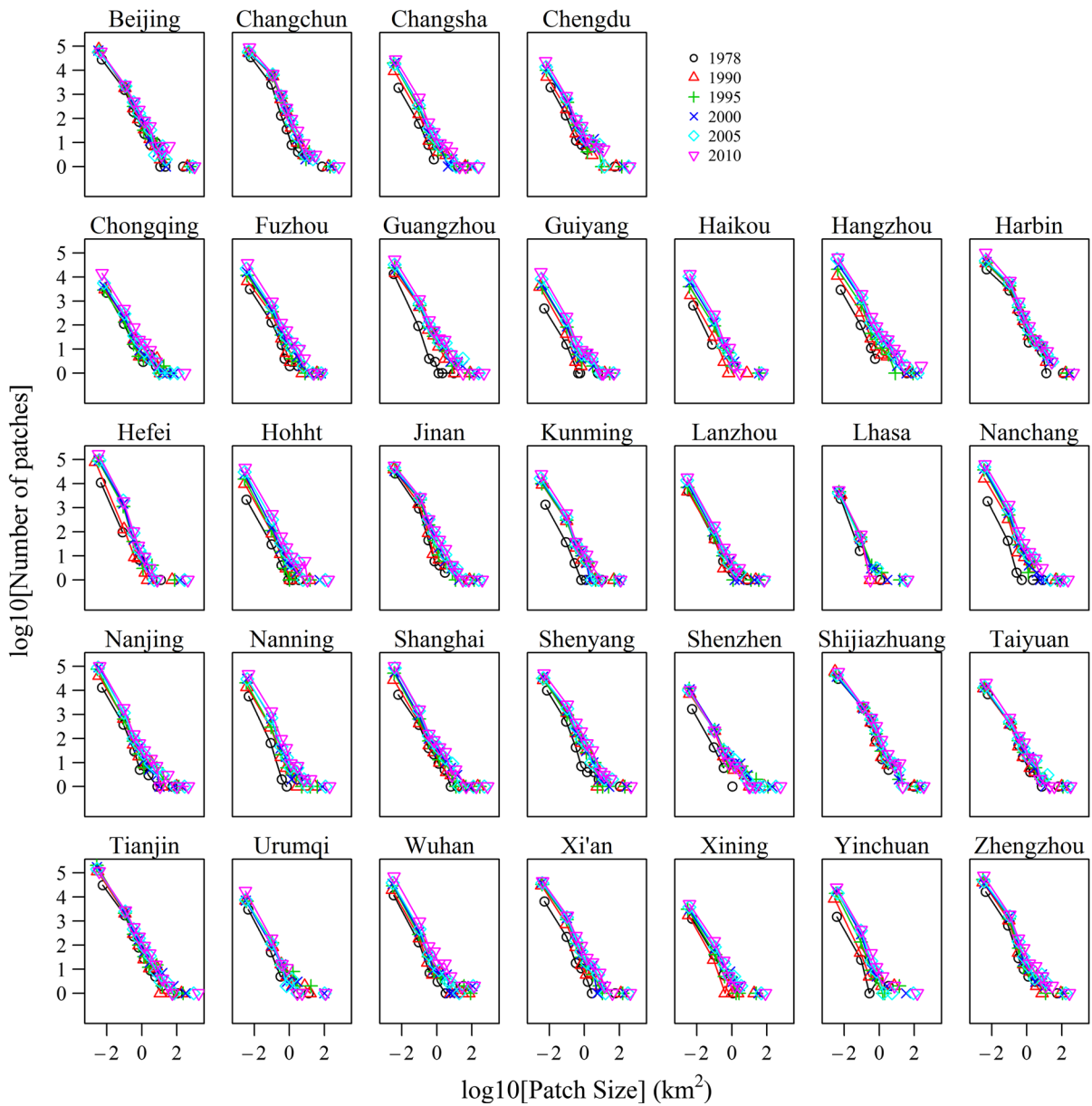


Fig. 4 The relationship between the number and the size of patches across cities and time periods

$$\alpha = 0.977 \log_{10}(A) - 1.063 \tag{5}$$

Plugging Eq. (5) into (4) and using the mean β (i.e., -1.29), we can derive a universal relationship for calculating the number of patches given the patch size and the total urban land area:

$$N = 0.0863S^{-1.29}A^{0.977} \tag{6}$$

The simulated patch numbers agreed well with observations across all cities, time periods, and patch sizes (Fig. 5).

The distribution of urban area along the patch size gradient showed a typical and consistent “V-shape” log–log pattern across cities and time periods (Fig. 6). The “V-shape” pattern was elevated over time along

Table 1 The largest patch sizes of urban land by city in 1978 and 2010

Patch size (km ²)	1978	2010
1–2	Haikou, Lasha, Shenzhen and Xining	
2–5	Hohhot, Nanning and Yinchuan	
5–10	Chongqing, Guangzhou, Guiyang, Kunming, Lanzhou and Nanchang	
10–20	Changsha, Hefei and Urumqi	
20–50	Fuzhou, Hangzhou and Wuhan	Lasha and Guiyang
50–100	Changchun, Chengdu, Jinan, Nanjing, Shijiazhuang, Taiyuan, Xi’an and Zhengzhou	Fuzhou, Haikou, Lanzhou and Xining
100–200	Harbin, Shanghai, Shenyang and Tianjin	Hohhot, Kunming, Nanning, Urumqi, Wuhan and Yinchuan
200–500	Beijing	Changsha, Chengdu, Chongqing, Guangzhou, Hangzhou, Harbin, Hefei, Jinan, Nanchang, Nanjing, Shenyang, Shijiazhuang, Taiyuan, Xi’an and Zhengzhou
>500		Beijing, Changchun, Shanghai, Shenzhen and Tianjin

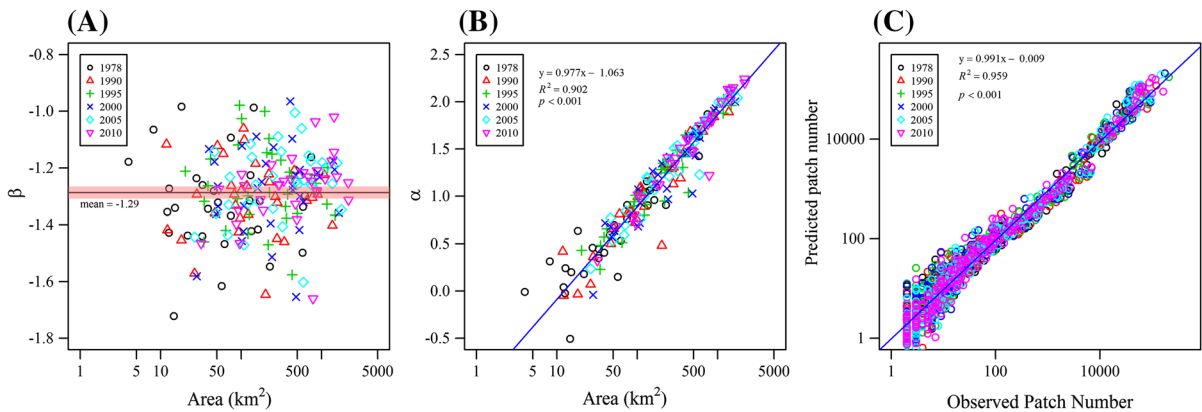


Fig. 5 Relationship between β and the total urban area (A), α and the total urban area (B), and comparison of predicted and observed number of urban land patches (C). The α and β values are the regression coefficients in the form of $\log_{10}(N) = \alpha + \beta \cdot \log_{10}(S)$ derived from all 32 cities and all time periods across China, each representing the hockey stick shaft shown in Fig. 4.

The number of patches (N) for a given patch size across all cities and time periods was predicted using $N = 0.0863S^{-1.29}A^{0.977}$ derived from this study (where S is the patch size and A is the total urban area)

the y axis or the area direction, suggesting the existence of urban expansion trends across all cities and an invariant area \sim patch size relationship over time. In addition, the patch sizes corresponding to the minimum total area as shown by the horizontal positions of the turning points of the “V-shape” varied considerably between 0.1 and 10 km² across cities and time periods. However, most of the minimum-area patch sizes were around 1 km².

Spatial patterns of urban growth

The relative fractions or composition of the three growth types (i.e., infilling, edge-expansion, and leapfrogging) in terms of patch number have experienced drastic changes since 1978, especially during the early period (Fig. 7). These fractions were strongly and linearly correlated during 1978–1990, and weakened during 1990–1995, and demonstrated no relationship

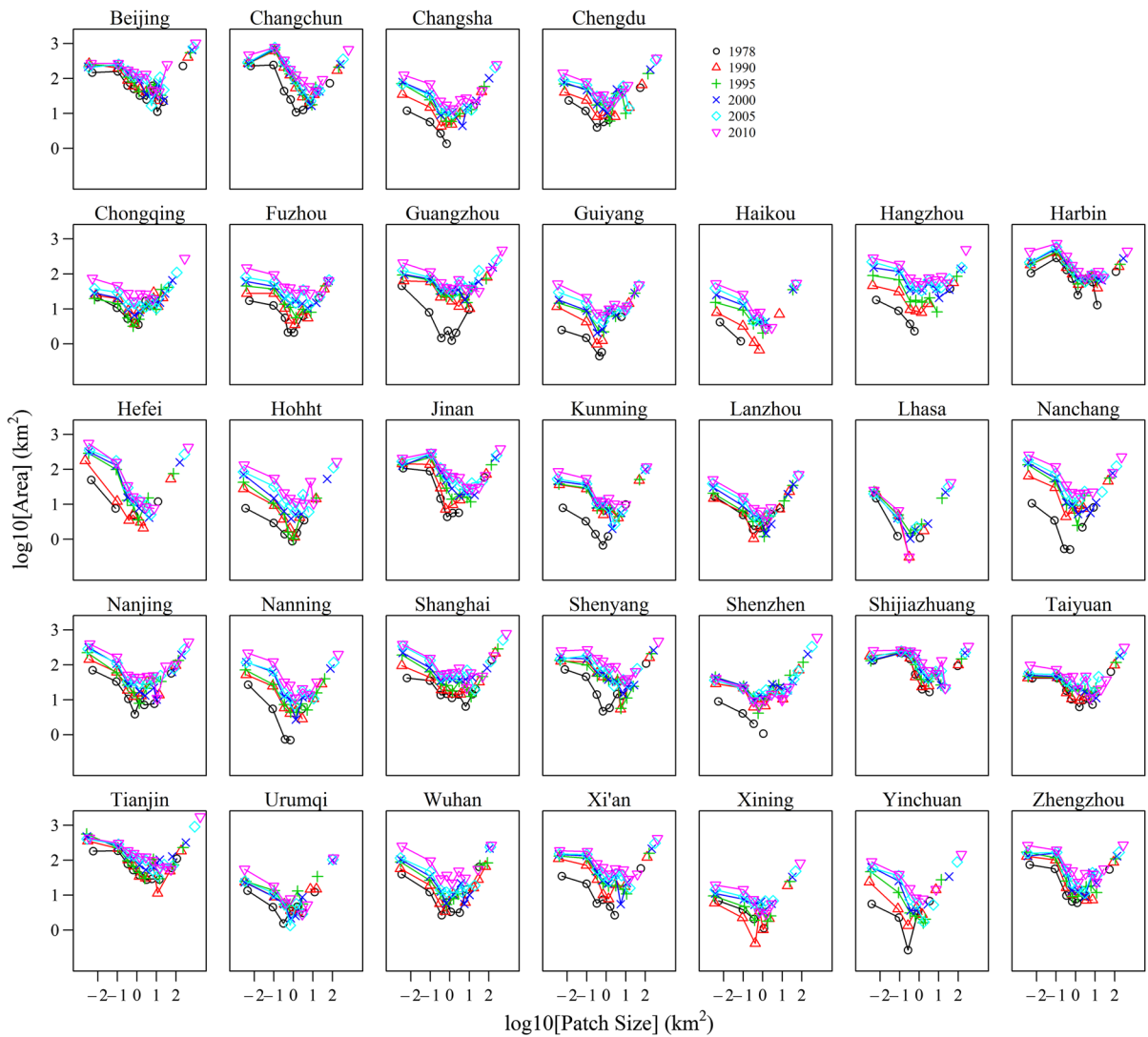


Fig. 6 The V-shape log–log relationship between patch size and associated total area

thereafter. The number of infilling has been the smallest among the three (Table 2). However, it has increased from 7.6 % on average during 1978–1990 to around 25 % during 2000–2005, followed by a decrease of 4.6 %. Its coefficient of variation (CV) has steadily decreased from 0.82 to about 0.30. The weight of edge-expansion in terms of patch number increased steadily from 24 % to about 40 % over time with a decreasing CV as well. In contrast, the fraction of leapfrogging patches accounted for 68 % of all patches during 1978–1990. It gradually decreased to 32 % during 2000–2005, and then rebounded to 39 %. The CV of leapfrogging weight across cities was relatively stable across time periods.

The relative fractions of the three growth types in terms of area also experienced substantial changes over time (Fig. S3; Table S3). The weight of infilling area doubled from 11 % during 1978–1990 to 22 % in 2000–2005, and then dropped to 17.5 % during the period after. Edge-expansion was the most extensive form of urban growth since 1990 (accounted almost half from 46 to 51 %), and it was leapfrogging before that. The fraction of leapfrogging in term of area has been shrinking from 47 % during 1978–1990 to 27 % in the period of 1990–2005, and then followed by an 8 % jump. The CV of edge-expansion fraction was the smallest among the three, and infilling the highest.

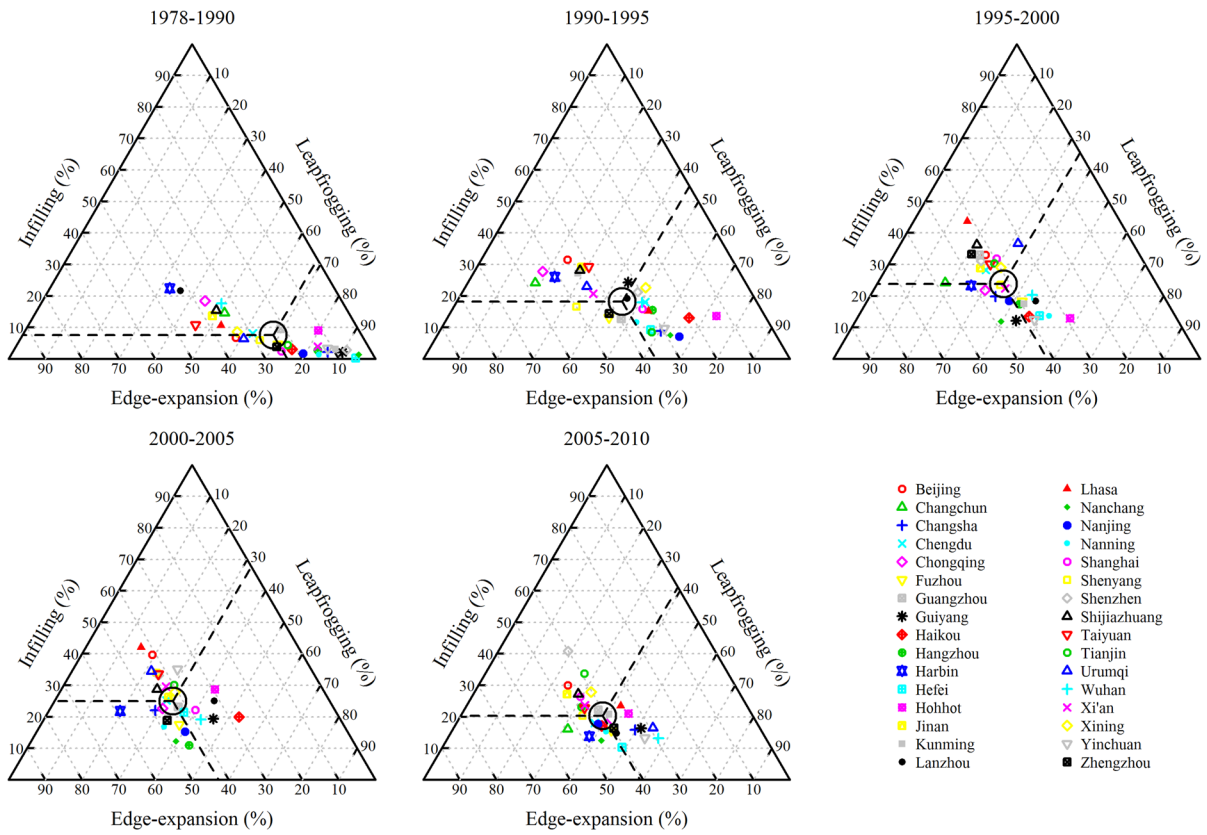


Fig. 7 The change of the proportional composition, calculated from their numbers of patches, of the three growth types (i.e., infilling, edge-expansion, and leapfrogging) with city and time.

The sum of the proportions equals to 100 %; the *large circle* represents the location of the intersection of the three means, shown by the *dashed lines*

Table 2 The mean fractions (%) and coefficient of variation (i.e., mean divided by standard deviations) of the three urban growth types in terms of patch number across 32 cities during various time periods

	Infilling		Edge-expansion		Leapfrogging	
	Mean	CV	Mean	CV	Mean	CV
1978–1990	7.6	0.82	24.1	0.51	68.3	0.26
1990–1995	18.2	0.4	36.6	0.26	45.1	0.33
1995–2000	23.8	0.36	41.7	0.13	34.5	0.31
2000–2005	25	0.31	42.8	0.16	32.3	0.28
2005–2010	20.4	0.33	40.9	0.13	38.8	0.24

In general, the number of infilling patches was frequently the fewest among the three growth types across cities and time periods (Table 3; Fig. 7). From 1978 to 1990, the number of infilling patches was consistently the smallest in all 32 cities. The

leapfrogging patches were the fewest among the three in 12 cities from 1995 to 2005. The number of leapfrogging patches was the largest across cities from 1978 to 1995, but took over by the number of edge-expansion since. The general statistics of the three types of growth in terms of area (Table S4) were similar to those of patches as described above except that the number of leapfrogging patches was the largest across cities from 1978 to 1990.

Table 4 lists the compactness index (CI) for each city across different time periods. The cities that had the highest CI were Beijing and Tianjin, and they appeared 4 and 3 times in the top 5 CIs, among the 32 cities, during the five time periods, respectively. On the other end, Guiyang, Haikou, Nanchang, and Yinchuan appeared four times in the bottom 5 CIs out of the five time periods. Overall, the CI increased from 0.18 in 1978–1990 to 0.31 in 2000–2005, and then dropped to 0.26 on average across all cities. As

Table 3 The frequency of minimum and maximum fraction appearance according to number of patches among three growth types in 32 individual cities

	Number of minimum fraction appearance			Number of maximum fraction appearance		
	Infilling	Edge-expansion	Leapfrogging	Infilling	Edge-expansion	Leapfrogging
1978–1990	32	0	0	0	2	30
1990–1995	26	1	5	0	11	21
1995–2000	19	1	12	2	20	10
2000–2005	20	0	12	0	26	6
2005–2010	28	0	4	1	18	13

Table 4 Compactness indexes for 32 major cities in China over the past three decades

City	Time periods					
	1978–1990	1990–1995	1995–2000	2000–2005	2005–2010	Mean
Beijing	0.18	0.39	0.40	0.40	0.34	0.34
Changchun	0.22	0.35	0.35	0.35	0.26	0.31
Changsha	0.16	0.17	0.32	0.35	0.21	0.24
Chengdu	0.20	0.22	0.32	0.31	0.22	0.25
Chongqing	0.24	0.39	0.29	0.23	0.22	0.27
Fuzhou	0.17	0.22	0.25	0.25	0.21	0.22
Guangzhou	0.31	0.18	0.38	0.29	0.29	0.29
Guiyang	0.10	0.32	0.20	0.25	0.19	0.21
Haikou	0.10	0.21	0.17	0.20	0.20	0.18
Hangzhou	0.12	0.21	0.26	0.20	0.28	0.21
Harbin	0.26	0.31	0.29	0.34	0.22	0.28
Hefei	0.06	0.19	0.24	0.31	0.19	0.20
Hohhot	0.13	0.10	0.21	0.32	0.25	0.20
Jinan	0.20	0.35	0.36	0.30	0.34	0.31
Kunming	0.11	0.38	0.27	0.30	0.24	0.26
Lanzhou	0.36	0.25	0.25	0.27	0.23	0.27
Lhasa	0.13	0.26	0.54	0.51	0.31	0.35
Nanchang	0.11	0.15	0.24	0.25	0.27	0.20
Nanjing	0.14	0.17	0.28	0.30	0.30	0.24
Nanning	0.12	0.22	0.22	0.29	0.23	0.22
Shanghai	0.17	0.22	0.35	0.24	0.36	0.27
Shenyang	0.17	0.30	0.30	0.37	0.24	0.28
Shenzhen	0.15	0.26	0.39	0.39	0.45	0.33
Shijiazhuang	0.23	0.37	0.40	0.30	0.28	0.32
Taiyuan	0.26	0.35	0.36	0.36	0.26	0.32
Tianjin	0.16	0.18	0.40	0.38	0.40	0.30
Urumqi	0.16	0.27	0.37	0.39	0.15	0.27
Wuhan	0.26	0.24	0.31	0.27	0.20	0.26
Xi'an	0.14	0.30	0.33	0.34	0.30	0.28
Xining	0.36	0.23	0.31	0.30	0.32	0.30
Yinchuan	0.11	0.15	0.17	0.35	0.21	0.20
Zhengzhou	0.17	0.25	0.40	0.28	0.22	0.26

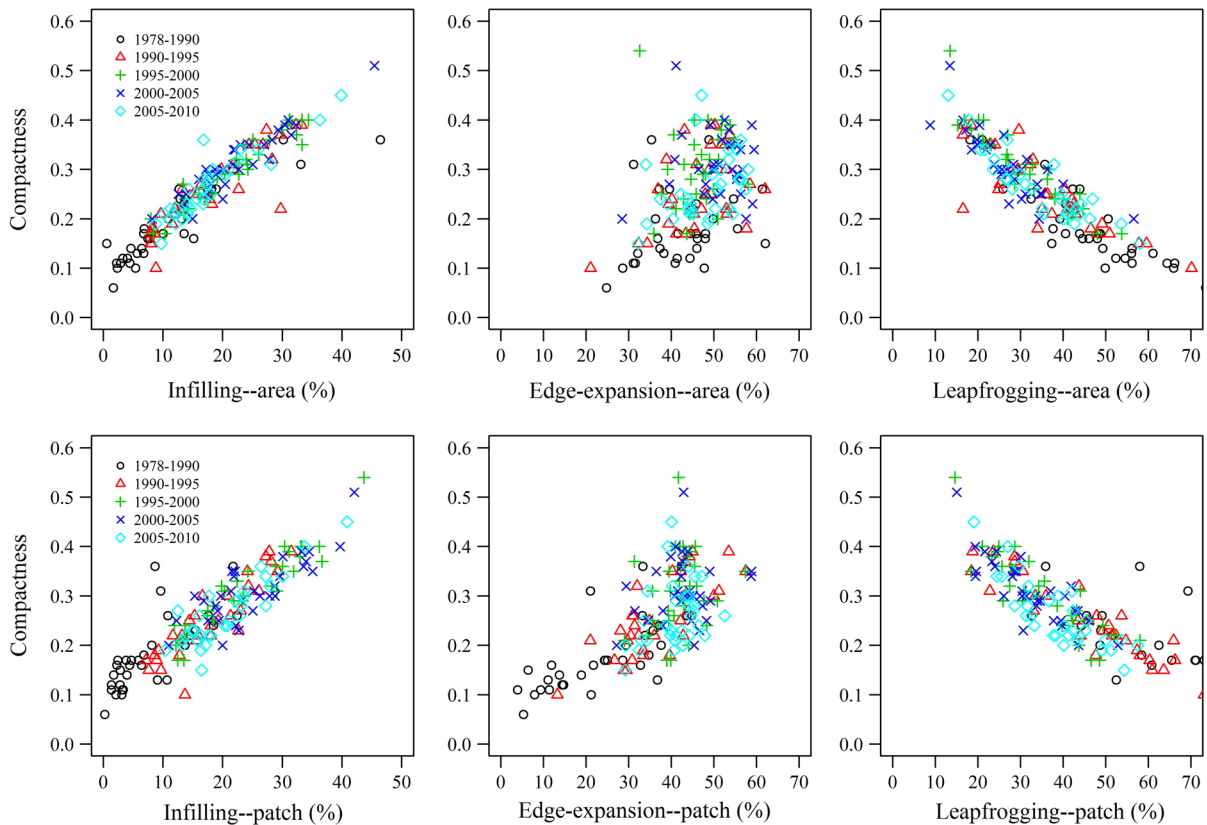


Fig. 8 Relationships between compactness index and urban growth types. The fractions of growth types were calculated based on either area or number of patches

expected from its formulae, CI had strong relationships with the fractions of various urban growth types regardless how the fractions were calculated from (Fig. 8). For example, it had a negative relationship with leapfrogging which has an E value of zero.

Discussion

Urbanization is both the consequence and the fuel of economic growth, and this is particularly true in China (e.g., Ding and Lichtenberg 2011; Bai et al. 2012; Cheung 2012; Bai et al. 2014; Wu et al. 2014). The urbanization processes, especially the rates, and spatial and temporal dimensions of urban land expansion, in China showed clear footprints of a series of economic reforms and national policies. China initiated its economic reform in the late 1970s with preferential focus on the development of the eastern region, especially coastal areas, and continued

targeting the eastern region for economic development but also concentrated on the central region for most of the 1980s and 1990s (Lai 2002). The fastest rates of urban expansion seen in the periods 1990–1995 and 2005–2010 were probably driven by the implementation of radical reforms after Deng Xiaoping’s southern tour in 1992 and a stable and relatively fast economic growth during these periods (Zhu 2012). The large variability of expansion rates observed during 1990–1995 also reflected the geographic variation of urban growth in the early phase of the economic reforms that favored economic growth and urban expansion in the coastal areas and eastern China. In the late 1990s, the central government launched western development strategy to promote development of western inland (Lai 2002; Schneider et al. 2005; Shue and Wong 2007). The highest average and peak annual expansion rates ($5.6 \pm 4.5\%$ and 16.7%) between 2000 and 2005 were observed in the western region, in contrast with $5.4 \pm 3.5\%$ and 11.9% in the central

region, and $4.9 \pm 1.7\%$ and 7.2% in the eastern region, which corresponds well to the implementation of western development policy in the late 1990s.

The influences of diverse socioeconomic and institutional changes on China's urban expansion can be further exemplified by our detailed comparative studies between or among different cities. For example, Chengdu and Chongqing, two large cities in Southwestern China, have undergone extensive expansion over the past three decades with an overall higher growth rate in Chengdu than Chongqing, but a much higher growth rate was observed in Chongqing since 1996 primarily driven by the establishment of Chongqing municipality in 1997 when a series of significant and preferential investment policies were authorized by the central and local government (Qu et al. 2014). Three capital cities in Northeast China (i.e., Shenyang, Changchun and Harbin) were once highly urbanized in China and then their urban expansion processes fell behind the southern coastal cities in the 1990s when the economic development in Northeast China was relatively low because of tremendous challenges from resource depletion, environmental pollution and business reconstructing. However, the "Revitalizing Old Industrial Base of Northeast China" strategy proposed in 2003, has promoted the economic recovery of the region and brought a brand new era of urbanization in the three cities when they all went through an abruptly rapid urban expansion since 2005 (Sun et al. 2014). The magnitude of urban expansion in the Jing-Jin-Ji Urban Agglomeration over the past three decades ranked as Tianjin, Beijing, and Shijiazhuang from high to low, related closely to the preferential policy for Binhai New Area development in Tianjin, Beijing's unique political privilege as the capital of China, and Shijiazhuang's physical location near Beijing suffering negative "shadow effect" (Wu et al. 2015).

Our patch analysis revealed three lines of evidence together pointed to a converged urban patch structure in China: the invariant scaling relationship between patch size and patch number, the typical "V-shape" log–log partitioning of urban area along the patch size gradient, and the existence of a single, large, central core in most of the cities. Most importantly, it was shown that the number of patches for a given patch size in any city can be predicted by a unified function of the patch size and the total urban area (i.e., Eq. 6). This universal function clearly suggests that the

number of patches decreases inversely and superlinearly (the scaling coefficient was smaller than -1) with patch size within all cities, and the ratio (γ) of the number of patches between two patch sizes with any given city in China can be expressed as:

$$\gamma = \frac{N_1}{N_2} = \left(\frac{S_2}{S_1} \right)^{1.29}$$

where N_1 and N_2 are the number of patches for patch sizes S_1 and S_2 , respectively. On the other hand, the ratio of patch numbers for the same patch size in different cities can be estimated by:

$$\gamma = \frac{N_1}{N_2} = \left(\frac{A_1}{A_2} \right)^{0.977}$$

where A_1 and A_2 are the urban land areas of the two cities, respectively. Although our study covered a wide variety of major cities in China and a relatively long time span of more than 30 years, it was interesting to see the existence of an invariant function that can unify the patch size and patch number relationship across time and space. We have not seen anything similar to this finding, and whether this relationship can be extrapolated into other regions remains to be seen.

Several processes might be responsible for the converged urban patch structure. First, the central government-led model of urban development in China could increase the similarity in the way of urbanization across various cities (Chan 2010), which can be supported by the fact that a similar convergent urban form was found in a study on urban land use change of four cities in the Pearl River Region in China (Seto and Fragkias 2005). Second, the trajectory of patch structure formation during urban development might be insensitive to the differences in geographic location, urbanization history, ecological context, economic development stage, and city size, and largely a spatial self-organization of urban land patches. Similarly, a high degree of similarity in spatiotemporal patterns of urbanization between two fastest growing metropolitan regions in the United States was observed (Wu et al. 2011). A hierarchical patch dynamics framework based study on spatiotemporal patterns of urbanization in the central Yangtze River Delta region, China from 1979 to 2008 showed that temporal trends in landscape pattern metrics derived from patch characteristics at three hierarchical levels

of the county, prefecture and region were similar (Li et al. 2013a). These further suggest the possible existence of a generally converged urban patch structure. Of course, more cross-boundary studies covering diverse socioeconomic regimes and biophysical conditions and across multiple space and time scales are required to test the universality of the observed convergence of urban patch structure in China.

Dietzel et al. (2005a) hypothesized that the general evolution of urban growth is a result of cyclic process of two alternate phases of diffusion and coalescence, and this hypothesis can be tested in light of the dynamic co-evolution of multiple landscape and urban growth metrics. Many previous investigations were conducted to test the generality of this urban growth hypothesis, a few confirmed diffusion-coalescence phase dynamics (Dietzel et al. 2005b; Xu et al. 2007), and some found that the urban development could experience the transition phase from diffusion to coalescence (Liu et al. 2010; Qu et al. 2014; Zhao et al. 2014) and others recognized the coexistence of diffusion and coalescence (Li et al. 2013a, b). The discrepancies among those studies can be related to the differences in temporal scale (over a 100 year time span or just several decades), spatial scale (data used with fine or coarse resolution and extent covering only urban core or including suburban and even exurban areas), and characteristics of the urbanization process (e.g., market-oriented or policy-led). It is more likely that a continuum process not dichotomy of diffusion and coalescence could better capture the urban development trajectory in real-world systems (Jenerette and Potere 2010; Tian et al. 2011; Li et al. 2013a), and this remains to be explored.

Our results generally supported the continuum of diffusion-coalescence urbanization process as three urban growth forms (infilling, edge-expansion and leapfrogging) coexisted during the course of the study period, and their composition shifted as urbanization progresses. Leapfrogging, which can increase both the area and the number of patches of urban land, resulting in a diffuse city, is the dominant form of urban expansion at the early stage of urbanization. Edge-expansion and infilling together are the dominant forms of urban expansion in the later stage, leading to a relatively compact city as they can expand the area of urban land but will not change the number of patches. During the course of the study period, the relative

patch number composition of infilling, edge-expansion, and leapfrogging for 32 China's major cities has evolved from 1:2:7 from 1978 to 1990 into a relatively stable ratio of 2:4:4 during the past 15 years or so, while their relative area composition from 1:4:5 to 2:5:3.

A compact urban expansion will lead to a smaller physical footprint of the cities thanks to its economic use of land and may result in subsequent less impacts on the environment relative to a diffuse one (Jenks et al. 1996; Jenks and Burgess 2000; Williams et al. 2000; Neuman 2005). However, on the other hand, a diffuse urban expansion may help maintain the remnant native habitat patches which will favour the conservation of native biodiversity in the city during urbanization (Wu et al. 2011). Substantial changes in growth types and compactness have been observed across cities and time periods in China. It is still a great challenge to define what is the sustainable form of cities for China. Nevertheless, it is prudent to believe that there does not exist a ubiquitous answer and it depends on the geographic location, economic development stage, the size of existing urban areas, and possible ecological, social and economic effects of urban expansion.

Conclusions

Spatially explicit comparative investigations on urban expansion among different cities are sorely lacking, especially across large geospatial extents. China's rapid urbanization in parallel with its economic boom over the past three decades has attracted worldwide attention. This study provided a comparative understanding on spatially explicit patterns and dynamics of urbanization in 32 major cities across China from 1978 to 2010.

Rapid urban expansion was observed in these 32 major cities during this time period, with an overall annual expansion rate of $6.8 \pm 2.5\%$. The sizes of cities were smaller and rates of expansion were slowed in the western region than those in the eastern and central regions in general due to regional disparities. However, the highest average and peak annual expansion rates were observed in the western region between 2000 and 2005, propelled by the implementation of a national policy targeted to promote western development in the late 1990s. It seems that Chinese urbanization is entering a new stage indicated by a

drastically narrowed difference in urban expansion rates among cities and an obvious cyclic dispersed urban expansion across all the cities during the period 2005–2010.

It is more likely that a continuum process not dichotomy of diffusion and coalescence could better capture the urban development trajectory in China's urbanization. A converged urban patch structure was found across cities and time periods in China although the differences in economic development, social and ecological contexts, and local policies were large. This structure was characterized by an invariant scaling relationship between patch size, patch number, and total urban area across cities in time and space, a "V-shape" log–log distribution of urban area along patch size gradient, and the existence of one single large urban core patch in most cities. However, more work is needed to test the universality of this relationship across regions and countries and to understand the implications to city organization, metabolism, and evolution.

Acknowledgments This study was supported by the National Natural Science Foundation of China (#31321061 and #41071050), and the 111 Project (B14001).

References

- Angel S, Sheppard SC, Civco DL, Buckley R, Chabaeva A, Gitlin L, Kraley A, Parent J, Perlin M (2005) The dynamics of global urban expansion. Transport and Urban Development Department, The World Bank, Washington, DC
- Bagan H, Yamagata Y (2012) Landsat analysis of urban growth: how Tokyo became the world's largest megacity during the last 40 years. *Remote Sens Environ* 127:210–222
- Bai XM, Chen J, Shi PJ (2012) Landscape urbanization and economic growth in China: positive feedbacks and sustainability dilemmas. *Environ Sci Technol* 46:132–139
- Bai XM, Shi PJ, Liu YS (2014) Realizing China's urban dream. *Nature* 509:158–160
- Bettencourt LMA, Lobo J, Helbing D, Kuhnert C, West GB (2007) Growth, innovation, scaling, and the pace of life in cities. *Proc Natl Acad Sci USA* 104:7301–7306
- Chan KW (2007) Misconceptions and complexities in the study of China's cities: definitions, statistics, and implications. *Eurasian Geogr Econ* 48:383–412
- Chan KW (2010) Fundamentals of China's urbanization and policy. *China Rev* 10:63–93
- Chen Y, Zhang Z, Du SQ, Shi PJ, Tao FL, Doyle M (2011) Water quality changes in the world's first special economic zone, Shenzhen, China. *Water Resour Res*. doi:10.1029/2011WR010491
- Cheung PTY (2012) China's changing regional development: trends, strategies and challenges in the 12th Five-Year Plan (2011–2015) period. *Asia Pacific Viewpoint* 53:1–6
- Deng JJ, Du K, Wang K, Yuan CS, Zhao JJ (2012) Long-term atmospheric visibility trend in Southeast China, 1973–2010. *Atmos Environ* 59:11–21
- Dietzel C, Herold M, Hemphill JJ, Clarke KC (2005a) Spatio-temporal dynamics in California's Central Valley: empirical links to urban theory. *Int J Geogr Inf Sci* 19:175–195
- Dietzel C, Oguz H, Hemphill JJ, Clarke KC, Gazulis N (2005b) Diffusion and coalescence of the Houston Metropolitan Area: evidence supporting a new urban theory. *Environ Plan* 32:231–246
- Ding CR, Lichtenberg E (2011) Land and urban economic growth in China. *Journal of Regional Science* 51:299–317
- Elvidge CD, Tuttle BT, Sutton PS, Baugh KE, Howard AT, Milesi C, Bhaduri BL, Nemani R (2007) Global distribution and density of constructed impervious surfaces. *Sensors* 7:1962–1979
- Ernoul L, Sandoz A, Fellague A (2012) The evolution of two great Mediterranean Deltas: remote sensing to visualize the evolution of habitats and land use in the Gediz and Rhone Deltas. *Ocean Coast Manag* 69:111–117
- Folke C, Jansson A, Larsson J, Costanza R (1997) Ecosystem appropriation by cities. *Ambio* 26:167–172
- Foody GM (2002) Status of land cover classification accuracy assessment. *Remote Sens Environ* 80:185–201
- Forman RTT (1995) Land mosaics: the ecology of landscapes and regions. Cambridge University Press, Cambridge, pp 43–80
- Frolking S, Milliman T, Seto KT, Friedl MA (2013) A global fingerprint of macro-scale changes in urban structure from 1999 to 2009. *Environ Res Lett* 8:024004. doi:10.1088/1748-9326/8/2/024004
- Grimm NB, Faeth SH, Golubiewski NE, Redman CL, Wu JG, Bai XM, Briggs JM (2008) Global change and the ecology of cities. *Science* 319:756–760
- Janssen LFF, Van der Wel FJM (1994) Accuracy assessment of satellite derived land-cover data: a review. *Photogramm Eng Remote Sens* 60:419–426
- Jat MK, Garg PK, Khare D (2008) Monitoring and modelling of urban sprawl using remote sensing and GIS techniques. *Int J Appl Earth Obs Geoinf* 10:26–43
- Jenerette GD, Potere D (2010) Global analysis and simulation of land-use change associated with urbanization. *Landscape Ecol* 25:657–670
- Jenks M, Burgess R (eds) (2000) Compact cities: sustainable urban forms for developing countries. E. & F.N. Spon, London
- Jenks M, Burton E, Williams K (eds) (1996) The compact city: a sustainable urban form?. E. & F.N. Spon, London
- Ji CY, Liu QH, Sun DF, Wang S, Lin P, Li XW (2001) Monitoring urban expansion with remote sensing in China. *Int J Remote Sens* 22:1441–1455
- Kalnay E, Cai M (2003) Impact of urbanization and land-use change on climate. *Nature* 423:528–531
- Lai HH (2002) China's Western development program: its rationale, implementation, and prospects. *Mod China* 28:432–466
- Li C, Li J, Wu JG (2013a) Quantifying the speed, growth modes, and landscape pattern changes of urbanization: a hierarchical patch dynamics approach. *Landscape Ecol* 28:1875–1888

- Li J, Li C, Zhu F, Song C, Wu JG (2013b) Spatiotemporal pattern of urbanization in Shanghai, China between 1989 and 2005. *Landscape Ecol* 28:1545–1565
- Lin GCS (2002) The growth and structural change of Chinese cities: a contextual and geographic analysis. *Cities* 19:299–316
- Liu JY, Zhan JY, Deng XZ (2005) Spatio-temporal patterns and driving forces of urban land expansion in China during the economic reform era. *Ambio* 34:450–455
- Liu XP, Li X, Chen YM, Tan ZZ, Li SY, Ai B (2010) A new landscape index for quantifying urban expansion using multi-temporal remotely sensed data. *Landscape Ecol* 25:671–682
- Lucas RE (1988) On the mechanics of economic development. *J Monet Econ* 22:3–42
- Luedeling E, Buerkert A (2008) Typology of oases in northern Oman based on Landsat and SRTM imagery and geological survey data. *Remote Sens Environ* 112:1181–1195
- Lv ZQ, Wu ZF, Wei JB, Sun C, Zhou QG, Zhang JH (2011) Monitoring of the urban sprawl using geoprocessing tools in the Shenzhen Municipality, China. *Environ Earth Sci* 62:1131–1141
- Mcdonald RI, Kareiva P, Forman RTT (2008) The implications of current and future urbanization for global protected areas and biodiversity conservation. *Biol Conserv* 141:1695–1703
- Mckinney ML (2002) Urbanization, biodiversity, and conservation. *Bioscience* 52:883–890
- Montgomery MR (2008) The urban transformation of the developing world. *Science* 319:761–764
- Neuman M (2005) The compact city fallacy. *J Plan Educ Res* 25:11–26
- Pedroni L (2003) Improved classification of Landsat thematic Mapper data using modified prior probabilities in large and complex landscapes. *Int J Remote Sens* 24:91–113
- Qu WY, Zhao SQ, Sun Y (2014) Spatiotemporal patterns of urbanization over the past three decades: a comparison between two large cities in Southwest China. *Urban Ecosyst*. doi:10.1007/s11252-014-0354-3
- Radeloff VC, Stewart SI, Hawbaker TJ, Todd J, Gimmi U, Pidgeon AM, Flather CH, Hammer RB, Helmers DP (2010) Housing growth in and near United States protected areas limits their conservation value. *Proc Natl Acad Sci USA* 107:940–945
- Saha AK, Arora MK, Csaplovics E GR (2005) Land cover classification using IRS LISS III image and DEM in a rugged terrain: a case study in Himalayas. *Geocarto Int* 20:33–40
- Schneider A, Mertes C (2014) Expansion and growth in Chinese cities, 1978–2010. *Environ Res Lett* 9(2):024008. doi:10.1088/1748-9326/9/2/024008
- Schneider A, Woodcock CE (2008) Compact, dispersed, fragmented, extensive? A comparison of urban growth in twenty-five global cities using remotely sensed data, pattern metrics and census information. *Urban Stud* 45:659–692
- Schneider A, Seto KC, Webster DR (2005) Urban growth in Chengdu, Western China: application of remote sensing to assess planning and policy outcomes. *Environ Plan* 32:323–345
- Schneider A, Friedl MA, Potere D (2009) A new map of global urban extent from MODIS satellite data. *Environ Res Lett* 4(4):044003. doi:10.1088/1748-9326/4/4/044003
- Seto KC, Fragkias M (2005) Quantifying spatiotemporal patterns of urban land-use change in four cities of China with time series landscape metrics. *Landscape Ecol* 20:871–888
- Seto KC, Sánchez-Rodríguez R, Fragkias M (2010) The new geography of contemporary urbanization and the environment. *Annu Rev Environ Resour* 35:167–194
- Seto KC, Fragkias M, Gueneralp B, Reilly MK (2011) A meta-analysis of global urban land expansion. *PLoS One* 6:e23777
- Seto KC, Güneralp B, Hutyra LR (2012) Global forecasts of urban expansion to 2030 and direct impacts on biodiversity and carbon pools. *Proc Natl Acad Sci USA* 109:16083–16088
- Shao M, Tang XY, Zhang YH, Li WJ (2006) City clusters in China: air and surface water pollution. *Front Ecol Environ* 4:353–361
- Shue V, Wong C (eds) (2007) *Paying for progress in China: Public finance, human welfare and changing patterns of inequality*. Routledge, London
- State Statistical Bureau (SSB) (2012) *China statistical yearbook*. China Statistics Press, Beijing (in Chinese)
- Stefanov WL, Ramsey MS, Christensen PR (2001) Monitoring urban land cover change: an expert system approach to land cover classification of semiarid to arid urban centers. *Remote Sens Environ* 77:173–185
- Sun C, Wu ZF, Lv ZQ, Yao N, Wei JB (2013) Quantifying different types of urban growth and the change dynamic in Guangzhou using multi-temporal remote sensing data. *Int J Appl Earth Obs Geoinf* 21:409–417
- Sun Y, Zhao SQ, Qu WY (2014) Quantifying spatiotemporal patterns of urban expansion in three capital cities in Northeast China over the past three decades using satellite data sets. *Environ Earth Sci*. doi:10.1007/s12665-014-3901-6
- Tan MH, Li XB, Xie H, Lu C (2005) Urban land expansion and arable land loss in China—a case study of Beijing-Tianjin-Hebei region. *Land Use Policy* 22:187–196
- Tian G, Jiang J, Yang ZF, Zhang YQ (2011) The urban growth, size distribution and spatio-temporal dynamic pattern of the Yangtze River Delta megalopolitan region, China. *Ecol Model* 222:865–878
- Trusilova K, Jung M, Churkina G, Karstens U, Heimann M, Claussen M (2008) Urbanization impacts on the climate in Europe: numerical experiments by the PSU-NCAR Mesoscale Model (MM5). *J Appl Meteorol Climatol* 47:1442–1455
- United Nations (2013) *World Urbanization Prospects: The 2012 Revision*. United Nations Department of Economic and Social Affairs, Population Division, New York
- Wang L, Li CC, Ying Q, Cheng X, Wang XY, Li XY, Hu LY, Liang L, Yu L, Huang HB (2012) China's urban expansion from 1990 to 2010 determined with satellite remote sensing. *Chin Sci Bull* 57:2802–2812
- Weng QH (2002) Land use change analysis in the Zhujiang Delta of China using satellite remote sensing, GIS and stochastic modelling. *J Environ Manag* 64:273–284
- Williams K, Burton E, Jenks M (eds) (2000) *Achieving sustainable urban form*. E. & F.N. Spon, London
- Wu JG (2014) Urban ecology and sustainability: the state-of-the-science and future directions. *Landsc Urb Plan* 125:209–221

- Wu JG, Jenerette GD, Buyantuyev A, Redman CL (2011) Quantifying spatiotemporal patterns of urbanization: the case of the two fastest growing metropolitan regions in the United States. *Ecol Complex* 8:1–8
- Wu JG, He CY, Huang GL, Yu DY (2013) Urban landscape ecology: Past, present, and future. In: Fu B, Jones KB (eds) *Landscape ecology for sustainable environment and culture*. Springer, Dordrecht, pp 37–53
- Wu JG, Xiang WN, Zhao JZ (2014) Urban ecology in China: historical developments and future directions. *Landscape Urb Plan* 125:222–233
- Wu WJ, Zhao SQ, Zhu C, Jiang JL (2015) A comparative study of urban expansion in Beijing, Tianjin and Shijiazhuang over the past three decades. *Landscape Urb Plan* 134:93–106
- Xu C, Liu M, Zhang C (2007) The spatiotemporal dynamics of rapid urban growth in the Nanjing metropolitan region of China. *Landscape Ecol* 22:925–937
- Yang XC, Hou YL, Chen BD (2011) Observed surface warming induced by urbanization in east China. *J Geophys Res*. doi:[10.1029/2010JD015452](https://doi.org/10.1029/2010JD015452)
- Yuan F, Sawaya KE, Loeffelholz BC, BE (2005) Land cover classification and change analysis of the Twin Cities (Minnesota) Metropolitan Area by multitemporal Landsat remote sensing. *Remote Sens Environ* 98:317–328
- Zhang C, Tian HQ, Chen GS, Chappelka A, Xu XF, Ren W, Hui DF, Liu ML, Lu CQ, Pan SF (2012) Impacts of urbanization on carbon balance in terrestrial ecosystems of the Southern United States. *Environ Pollut* 164:89–101
- Zhao SQ, Da LJ, Tang ZY, Fang HJ, Song K, Fang JY (2006) Ecological consequences of rapid urban expansion: Shanghai, China. *Front Ecol Environ* 4:341–346
- Zhao JJ, Chu C, Zhao SQ (2014) Comparing the spatiotemporal dynamics of urbanization in Nanjing and Xi'an of China over the past three decades. *J Urb Plan Dev*. doi:[10.1061/\(ASCE\)UP.1943-5444.0000251](https://doi.org/10.1061/(ASCE)UP.1943-5444.0000251)
- Zhou LM, Dickinson RE, Tian YH, Fang JY, Li QX, Kaufmann RK, Tucker CJ, Myneni RB (2004) Evidence for a significant urbanization effect on climate in China. *Proc Natl Acad Sci USA* 101:9540–9544
- Zhou DC, Zhao SQ, Zhu C (2012) The Grain for Green Project induced land cover change in the Loess Plateau: a case study with Ansai County, Shanxi Province, China. *Ecol Ind* 23:88–94
- Zhu XD (2012) Understanding China's growth: past, present, and future. *J Econ Perspect* 26:103–124